00-70

Environment Canada

Water Science and Technology Directorate

Direction générale des sciences et de la technologie, eau

Environnement Canada

Application of a Two-Dimensional Hydrodynamic Reservoir Model to Lake Erie

By:
L. Boegman, M. Loewen, P. Hamblin, D. Culver...

00-70

March 20, 2000

Application of a Two-Dimensional Hydrodynamic Reservoir Model to Lake Erie

L. Boegman[1] and M. R. Loewen[2,3]

Environmental Fluid Dynamics Laboratory
Department of Mechanical and Industrial Engineering, University of Toronto
Toronto, Ontario, M5S 3G8 CANADA

P. F. Hamblin

Aquatic Ecosystems Restoration Branch, National Water Research Institute
Burlington, Ontario, L7R 4A6 CANADA

D. A. Culver

Department of Evolution, Ecology, and Organismal Biology, Ohio State University
Columbus, Ohio, 43210 U.S.A.

M. N. Charlton

Aquatic Ecosystems Restoration Branch, National Water Research Institute
Burlington, Ontario, L7R 4A6 CANADA

NWRI Cont. # 00-70

[1] Present address: Department of Environmental Engineering, Centre for Water Research, University of Western Australia, Nedlands WA 6907, Australia.
[2] Present address: Department of Civil and Environmental Engineering, University of Alberta, Edmonton, Alberta, T6G 2G7 CANADA.
[3] Corresponding author.

MANAGEMENT PERSPECTIVE

In response to the rapid changes in the ecosystem of the Lake Erie and the need to prioritize the present and emerging issues, this mathematical modelling of the lake's hydrodynamical and water quality regime was undertaken.

This document reports on the surface meteorology, currents and the current state of coupled hydrodynamical and water quality modelling of Lake Erie.

These results will be disseminated to a broad audience of the internation aquatic science and Great Lakes communities through the journal publication .

Abstract

The relative impacts of changes in nutrient loading and zebra mussel establishment on plankton in large lakes are strongly influenced by hydrodynamics, yet adequately modelling the temporal/spatial complexity of physical and biological processes has been difficult. We adapted a two-dimensional public domain model, CE-QUAL-W2, to test whether it could provide a hydrodynamically accurate simulation of the seasonal variation in the vertical-longitudinal water quality of Lake Erie. We modeled hydrodynamics, nutrient concentrations, dissolved oxygen, and algal abundances, but not zooplankton or zebra mussels, using meteorological forcing functions, water inflows/outflows and nutrient loadings. To calibrate and validate the model, predictions were compared to an extensive set of field data. The model accurately predicted water level fluctuations without adjustment. However, significant modifications to the eddy coefficient turbulence algorithm were required in order to predict acceptable longitudinal currents. The thermal structure and dissolved oxygen levels were accurately predicted in all three basins, even though this laterally averaged model cannot simulate Coriolis effects. We are currently extending the model to include the effects of zebra mussels and zooplankton.

SOMMAIRE À L'INTENTION DE LA DIRECTION

Pour répondre à l'évolution rapide de l'écosystème du lac Érié et à la nécessité de prioriser les problèmes présents et nouveaux, on a entrepris une modélisation mathématique du régime hydrodynamique et de la qualité de l'eau de ce lac.

Ce document fait rapport sur la météorologie à la surface, les courants et l'état actuel de la modélisation couplée de l'hydrodynamique et de la qualité de l'eau de l'eau du lac Érié.

Ces résultats seront diffusés grâce à leur publication dans le Journal, à une large audience des Grands Lacs et de scientifiques du monde entier spécialisés en sciences aquatiques.

Résumé

Dans les grands lacs, les impacts relatifs sur le plancton des changements dans la charge en nutriants et de l'installation des moules zébrées sont fortement influencés par l'hydrodynamique; cependant il est difficile de modéliser correctement la complexité spatio-temporelle des processus physiques et biologiques. Nous avons adapté un modèle bidimensionnel du domaine public, le CE-QUAL-W2, afin de tester s'il pouvait fournir une simulation hydrodynamique exacte de la variation saisonnière de la qualité de l'eau selon les axes verticaux et longitudinaux. Nous avons modélisé l'hydrodynamique, les concentrations de substances nutritives, l'oxygène dissous et l'abondance des algues, mais pas le zooplancton ni les moules zébrées, en ayant recours aux fonctions de forçage météorologique, aux débits entrants et sortants de l'eau et aux charges en nutriants. Afin de calibrer et de valider ce modèle, des prédictions ont été comparées à un grand ensemble de données recueillies sur le terrain. Ce modèle a permis de prédire de façon exacte les fluctuations du niveau de l'eau sans nécessité d'ajustements. Mais il a fallu modifier largement l'algorithme de turbulence du coefficient d'Austausch pour prédire des courants longitudinaux acceptables. La structure thermique et les concentrations d'oxygène dissous ont été correctement prédites dans les trois bassins, même si ce modèle à faible moyennage latéral ne peut pas simuler les effets de la force de Coriolis. Nous sommes actuellement en train d'élargir le modèle afin d'inclure les effets des moules zébrées et du zooplancton.

Introduction

The water quality of Lake Erie deteriorated dramatically from the 1950s to 1970s due to eutrophication that was particularly strong in the western basin. In the 1970s, joint Canadian and United States legislation mandated tertiary treatment of municipal wastewater and implemented agricultural programs to reduce farm run-off. Lake Erie water quality improved and significant phytoplankton reductions in the western basin were observed (Nicholls *et al.*, 1977). In 1988, the discovery of filter-feeding zebra mussels (*Dreissena polymorpha*) in the lower Great Lakes and their subsequent proliferation (Berkman *et al.*, 1998) created a potential for further reductions in phytoplankton biomass and increased water clarity (Holland, 1993, Leach, 1993, Nicholls and Hopkins, 1993). Numerous mathematical models have been used to examine the hydrodynamics and nutrient/plankton/zebra mussel dynamics of Lake Erie; however, models published to date have been either physically based (Ivey and Patterson 1994 and Kuan, 1995) or biological / nutrient based (Madenjian, 1995 and Arnott and Vanni, 1996). Laboratory and field studies have shown that fully understanding the relative roles of changes in nutrient loading and zebra mussels on large, natural lakes like Lake Erie requires models that couple hydrodynamics and the dynamics of water quality and biota (Fréchette *et al.*, 1989). The problem involves adequately modeling the complexity of physical and biological processes in time and space, with sufficient computational efficiency that long-term trends in water quality may be economically simulated.

For an example of a physically based model, a one-dimensional thermodynamic model, DYRESM, was successfully used to model the vertical mixing for one month in the central basin of Lake Erie (Ivey and Patterson, 1984). At their mid-central basin sampling location, the lake is relatively vast, has a uniform depth and horizontal isotherms throughout the simulation period.

Under such conditions, horizontal advection was found to have a negligible effect upon temperature. However, all field observations were averaged over 48h because DYRESM is not capable of simulating the strong external (barotropic) seiches that oscillate along the lake's longitudinal axis. Mixing coefficients, identical to those used in prior simulations of much smaller water bodies, were found to adequately describe the vertical turbulent processes.

Another example is the three-dimensional hydrodynamic model, the Princeton Ocean Model, which was applied to Lake Erie for a 150-day summer simulation on a Cray super computer (Kuan, 1995). Using a σ- system coordinate, Kuan's model had 14 vertical levels varying in thickness from six meters in the eastern basin to 0.0375 meters in the western basin. Barotropic motions were reproduced leading to accurate water level predictions. Central and eastern basin currents were simulated satisfactorily in both phase and magnitude. A strong correlation was found between the accuracy of the predicted currents and the quality of the applied meteorological forcing field. Lake surface temperatures and fully mixed water columns were reproduced to within an average of 1°C over the entire simulation; however, during stratification, the model under- and over-predicted epilimnetic and hypolimnetic temperatures, respectively. The model failed to reproduce a distinct thermocline structure and central basin hypolimnion throughout the summer period and this was hypothesized to be a result of coarse vertical grid resolution.

The primary goal of this study was to test whether a two-dimensional model could provide a hydrodynamically accurate simulation of the seasonal variation in the vertical-longitudinal water quality of a large lake such as Lake Erie. For this study, the two-dimensional public domain model, CE-QUAL-W2, was chosen as it contains a fully predictive coupled water quality and hydrodynamic model that runs in a reasonable amount of time (~1 hr) using a

FORTRAN compiler on a personal computer. It includes hydrodynamics, nutrient concentrations, dissolved oxygen, and algal abundances, but not zooplankton or benthic grazers (e.g. zebra mussels). This two-dimensional model resolves the longitudinal and vertical axes and is therefore suited for application to relatively long, narrow water bodies, such as Lake Erie. The longitudinal dimension is aligned with Lake Erie's longest axis, which corresponds to the direction of the hydraulic flow and strongest seiching. Nutrient concentration, plankton biomass, thermal and bathymetric gradients are also strongest in this direction (Charlton, 1994). The vertical thermal structure must be accurately modelled because of its important influence on vertical mixing and hence, on the vertical distribution of nutrients and algae. This is especially important because ultimately the model will be used to estimate the algal availability to benthic feeding zebra mussels. Previous applications of CE-QUAL-W2 have been limited to small reservoirs, e.g. a thermal and dissolved oxygen application to DeGray Lake, Arkansas (Martin 1988) and modeling combined sewer overflow in Cheatham Lake, Tennessee (Adams *et al.*, 1997). To our knowledge, this is the first application of CE-QUAL-W2 to a large, natural lake. Work is in progress to incorporate zebra mussels and zooplankton into CE-QUAL-W2's model framework, allowing consideration of the effects of longitudinal and vertical mixing on nutrient availability and the relative influence of reductions in phosphorus and the introduction and proliferation of zebra mussels on the dramatic changes in Lake Erie's water quality.

We have modified CE-QUAL-W2 to make it applicable to a large wind driven lake and then hydrodynamically calibrated it for Lake Erie (Fig. 1), using water levels, horizontal currents, dissolved oxygen concentrations, and temperatures from an extensive field data set from May through September 1994. The empirical nature of the turbulence scheme made it necessary to separately calibrate the model to the observed data in each of the three basins.

Physical Characteristics

Lake Erie is of elongate form with a 6:1 aspect ratio of the main axis to the mean breadth. Lake Erie can be subdivided into three distinct physiographic basins: western, central and eastern with average depths of 10, 25 and 50 meters, respectively (Fig. 1,2). The western and central basins are separated by a rocky chain of islands following the 10 m depth contour from Point Pelee, Ontario to Marblehead, Ohio. The Pennsylvania Ridge, a low, wide submerged sand and gravel ridge, separates the eastern and central basins, extending from Long Point, Ontario to Erie, Pennsylvania (Schertzer & Hamblin, 2000).

A decrease in the depth-averaged temperature is observed when moving from the shallow well-mixed western basin to the seasonally stratified central and eastern basins. The sharp thermocline formed in the central basin can act as a vertical barrier to exchange between the epilimnion and hypolimnion and lead to anoxic conditions in the central basin hypolimnion (Charlton, 1980). East/west hypolimnetic transport across the Pennsylvania Ridge can affect temperature, nutrient and oxygen concentrations in the central basin hypolimnion. Increased winds during late summer and early fall result in a deepening of the thermocline and eventual breakdown of the summer thermal stratification.

Surface gravitational seiches with typical amplitudes of 10-30 cm are ubiquitous on Lake Erie. The periods of the lowest four natural seiche modes are 14.38, 9.14, 5.93 and 4.15-h (Platzman and Rao, 1964). Boyce and Chiocchio (1987) found that in Lake Erie's central basin the inertial (0.056 cph) and first mode (0.07 cph) currents dominated the observed energy spectra. Smaller peaks were seen at the diurnal (0.042 cph) and 0.01 cph (100-h) frequencies, while the second and third modes contained little energy. Saylor and Miller (1987) observed that inertial currents were most prominent in the deep water of the eastern basin, while central basin

internal currents were not as well defined. Hamblin (1987) found that storm surges in Lake Erie are associated with strong cyclonic disturbances traveling northeast and centered over the Great Lakes. He also observed that the amplitude of the storm surge set-up could exceed 2 m and that water levels generally return to normal within one day.

Methods

Model Description

The model bathymetry was specified using a digital 2 km bathymetric grid of Lake Erie obtained from the National Atmospheric and Oceanic Administration (NOAA; www.glerl.noaa.gov/data/bathy.html). In order to obtain a better fit to the shoreline, the NOAA grid is aligned 27.33° counter-clockwise from the central meridian of NOAA bathymetric chart 14820. In this two-dimensional application, the NOAA grid was laterally averaged into 65 vertical layers spaced at one-meter intervals and 222 longitudinal segments in ascending order from west to east (Fig. 2). A unique width is specified for each node and depths are relative to the Great Lakes Datum of 1985. Segments 65 to 222 (central and eastern basins) are spaced at 2000 m intervals and oriented along the longitudinal axis of the NOAA grid (27.33° counter-clockwise from the chart central meridian); to account for the "angled" nature of the western basin to that axis, segments 1 to 52, spaced at 1414 m intervals, are oriented 162.33° counter-clockwise from the chart central meridian; segments 53 to 64 (triangle from Sandusky, Ohio, to Point Pelee, Ontario to Lorain, Ohio) are spaced at 1779 m intervals and are transitionally oriented between western and central basin segments. Long Point Bay (Fig. 1), which averages 1 to 8 m in depth, was filled in west of the tip of Long Point, Ont., to correctly represent the

constriction in lake width due to Long Point. This bathymetric modification can be considered negligible, reducing total lake volume by ~0.3%.

CE-QUAL-W2 solves for the hydrodynamic variables by the direct solution of six fundamental equations and six unknowns. The governing equations, laterally and layer averaged, are: the horizontal momentum equation, the constituent/heat transport equation, the free water surface elevation equation, the hydrostatic pressure equation, the continuity equation, and the equation of state. The six unknowns are: water surface elevation, pressure, horizontal velocity, vertical velocity, constituent concentration/temperature and density. Lateral averaging eliminates the lateral momentum balance, lateral velocity and the Coriolis acceleration (Cole and Buchak, 1995).

The equations and unknowns are solved using a first-order, upwinded, finite-difference scheme, applied to a fixed grid of variable node spacing. A z-level vertical co-ordinate system is used. Explicit formulation of the effects of vertical eddy viscosity (A_z) on horizontal velocities necessitates a time step (Δt) restriction for physically realistic results:

$$\Delta t < \Delta z^2 / A_z \qquad (1)$$

where A_z is the local vertical grid point spacing. For large applications, this restriction can severely limit the feasible A_z range while maintaining reasonable run times. Hydrostatic stability is maintained through auto-stepping, which is an algorithm that calculates the maximum global time-step based upon the application of equation 1 at each node. Surface heat exchange is calculated using an explicit term-by-term process from incident short wave radiation, wind speed, air temperature, dew point temperature, cloud cover and water surface temperature. The sediment/water heat flux was set to zero as in a lake as large as Lake Erie it is considered to be negligible. Density instabilities are smoothed by setting the local vertical eddy diffusivity to 1000

m^2/s, resulting in vertical mixing of adjacent layers during the next timestep. Water densities are calculated based upon water temperature and solids concentration (Gill, 1982).

Shear production at the lake bed (τ_{bed}) is calculated using the Chézy coefficient (C_z) which is inversely proportional to the bottom roughness. Bottom shear is calculated as:

$$\tau_{bed} = \frac{g}{C_z^2} U|U| \tag{2}$$

where g is the gravitational constant and U is the longitudinal, laterally averaged velocity.

Input Data

Meteorological forcing parameters are applied uniformly to each finite difference segment along the lake or reservoir's surface. In the original model, these parameters were: air temperature, relative humidity, wind speed, wind direction, cloud cover and short-wave solar radiation which is calculated from latitude, sun angle and cloud cover. For this study, the following meteorological data were supplied by the National Water Research Institute (NWRI), Burlington, Ontario: air temperature, dew point temperature, wind speed, wind direction and incident short-wave solar radiation. Air temperature and wind speed data (Table 1) were recorded at 10-minute intervals by meteorological buoys (MET3 climate buoy) deployed in each of the three basins (Fig. 1). We modified the source code and input files of CE-QUAL-W2 to directly read the short-wave radiation values. Cloud cover measurements were not available and therefore were estimated by regression from the daily short-wave radiation (TVA, 1972).

Due to the size of Lake Erie and spatially varying meteorological conditions, the surface forcing values from each of the three meteorological stations were interpolated to apply unique surface-forcing conditions to each longitudinal segment (Boegman, 1999). Gaps in data series due to instrument failure or maintenance were overcome by substitution of data from adjacent

buoys. Failure of western and central basin radiometers required the use of eastern basin short-wave solar radiation data for the entire lake.

Water inflows and nutrient loadings were specified for the Grand (Ontario), Maumee, Sandusky and Detroit Rivers as well as the Cleveland Easterly, Cleveland Westerly, Toledo (Ohio) and Erie (Pennsylvania) wastewater treatment plants. Outflows were specified for the Welland Canal and Niagara River (Table 1). All variables were sampled daily, with the exception of the Grand River water temperatures which were sampled at a frequency greater than or equal to bi-weekly.

Observed water level time series were obtained from NOAA gauges that recorded water levels hourly at Toledo and Buffalo. Current meter data (EG&G and SACM3 meters with ±1cm/s and ±5° error), provided by NWRI for the central and western basin sampling locations (Fig. 1), were used to calibrate the modelled longitudinal currents. NWRI also provided temperature time series data using Brankner and Neil Brown temperature loggers deployed from meteorological buoys in all three basins (Fig. 1) as well as 638 temperature and dissolved oxygen profiles taken using a Seabird profiler at various lake locations from 20 May through 13 September 1994.

Original Vertical Eddy Viscosity Algorithm

Empirically derived eddy coefficients were used to model turbulence. The horizontal dispersion coefficients for momentum (A_x) and temperature/constituents (D_x) are assumed to be time- and space- invariant and are set equal to 1 m^2/s. In the vertical dimension, the diffusion coefficients' ad hoc representation does not have a strong theoretical basis and subsequently relies heavily on field data for adjustment and calibration. The vertical diffusion coefficients for

momentum (A_z) and temperature/constituents (D_z) vary in space and time and are computed locally by the model at each time step.

The vertical eddy viscosity (A_z) is formulated by analogy to the three-dimensional case (Cole & Buchak, 1995):

$$A_z = k\left(\frac{l^2}{2}\right)\sqrt{\left(\frac{\partial U}{\partial z}\right)^2 + \left(\frac{\partial V}{\partial z}\right)^2}\, e^{-CRi} \tag{3}$$

where k is the von Karman constant, l is a vertical length scale taken as the vertical grid point spacing, U is the longitudinal velocity, V is the lateral velocity, Ri is the local Richardson number and C is a constant taken as 1.5.

The longitudinal-vertical nature of this two-dimensional model causes the lateral velocity and its vertical gradient ($\partial V/\partial z$) to be zero. To account for this it is assumed that the effect of cross-wind shear ($\tau_{wind\text{-}y}$) on A_z is to generate a lateral wind wave component (Cole & Buchak, 1995) such that:

$$A_z = k\left(\frac{l^2}{2}\right)\sqrt{\left(\frac{\partial U}{\partial z}\right)^2 + \left(\frac{\tau_{wind-y} e^{-2kz}}{A_z}\right)^2}\, e^{-CRi} \tag{4}$$

where the A_z on the right hand side of equation 4 is the explicit value determined in the previous timestep. The resultant vertical eddy viscosities are exponentially damped with depth from the wind dependent surface value thus approaching zero at the lake bed. A_z is reduced in stratified regions based upon the local Richardson number. To prevent excessive run times (see equation 1), A_z was initially limited numerically such that:

$$1.4\text{x}10^{-6}\ \text{m}^2/\text{s} < A_z < 10^{-4}\ \text{m}^2/\text{s} \tag{5}$$

In figure 3a-c longitudinal currents modelled using the original A_z algorithm are compared with the observed longitudinal currents at 3, 11, and 24 m at central basin station C. However, one observes that the modelled currents have a spectral energy content 1.5 orders of magnitude greater than the field-observed currents at a frequency of 0.01 cph (Fig. 3d-f), and exhibit a large-amplitude low-frequency oscillation, characteristic of an undamped internal seiche (Fig. 3a-c). As a result, subsurface temperatures were under predicted by as much as 12°C in the central and western basins (Figs. 4-a and 4-b). Given that surface temperatures were correctly simulated, this suggests that the model incorrectly estimates the inter-basin exchange flow of cold, hypolimnetic water.

Modified Vertical Eddy Viscosity Algorithm

The undamped proliferation of internal seiches in large lakes results from incorrect specification of the turbulent processes governing dissipation of wind energy (Saggio and Imberger, 1998). These processes include the dissipation of basin-scale currents through shear production in the benthic boundary layer, non-linear decay of internal waves to higher modes, and the subsequent shoaling and breaking of internal waves as they impinge on sloped boundaries at the depth of the metalimnion. Poor spatial resolution and the hydrostatic approximation prevent the physical realization of these turbulent processes within CE-QUAL-W2's original eddy coefficient model framework. Further, Coriolis forces are significant in Lake Erie which has a width greater than 100 km, many times the ~ 5 km internal Rossby radius of deformation (Gill, 1982). As a result momentum transfer from the longitudinal to transverse direction could be acting to reduce the strength of observed longitudinal seiches.

As a result, ad hoc adjustments were made to the A_z algorithm until optimal agreement with the 1994 temperature and current data was obtained. The upper A_z bound (eq. 5) was

increased from 10^{-4} to 10^{-2} m^2/s, which reduced the modelled surface currents to the same order of magnitude as those observed (Fig. 5a) and to approximately 2-3% of the wind speed, in accordance with Gill (1982). Epilimnetic A_z values have been measured in an off-shore zone of the central basin (McCune, 1998), ranging from $3x10^{-4}$ m^2/s in light winds to $4x10^{-2}$ m^2/s during a storm event, and in a high-energy near-shore zone of the western basin ranging from 10^{-4} to 10^{-2} m^2/s (W. Edwards, Dept. of Evolution, Ecology, and Organismal Biology, Ohio State University, personal communication), so these range modifications are reasonable.

A_z was then linearly interpolated from the surface value to a wind-dependent range of 0.05 to 0.1 m^2/s in the benthic boundary layer. This is an increase of five orders of magnitude from the original turbulence scheme, which had predicted benthic A_z values of from $1.4x10^{-6}$ to 10^{-5} m^2/s. The source code was modified such that the Richardson number reduction was only applied when vertical density differences between layers were in excess of 0.01 kg/m^3. These changes significantly improved the modelled central basin longitudinal current at 11 m, reducing the strength of the 0.01 cph oscillation (Fig. 5b), but not at 24 m (Figs. 5c and 5f). Note that Lake Erie is 25 m deep at this central basin site. McCune (1998) observed that the maximum value of A_z in the central basin hypolimnion was approximately 10^{-5} m^2/s, suggesting that the A_z values calculated for this basin using the original A_z algorithm were reasonable. However, increasing the value of A_z through the metalimnion and hypolimnion (Table 2) can be justified in that it accounts for the dissipative processes (shear production, non-linear decay, and shoaling, etc.) that an eddy viscosity turbulence model cannot reproduce.

These modifications to A_z resulted in a reduction of the timestep from 600 s to 2 s (see equation 1) and an increase in runtime from 1 h to 1 wk. It was therefore necessary to remove the timestep restriction by making the effects of the A_z on horizontal velocity implicit (Boegman,

1999). Specifically, mixing coefficients for momentum and mass are assumed to be unequal. The vertical eddy diffusivity (D_z) is calculated as a fraction of A_z by dividing by the turbulent Prandtl number (P_r):

$$D_z = \hat{A}_z/P_r \tag{6}$$

where $\hat{A}_z$ is the vertical eddy viscosity computed using the original algorithm (Equation 4).

Results from a sensitivity analysis (Boegman, 1999) showed that the optimal values for P_r were 2.0 in the western and central basins and 7.0 in the eastern basin. Note, that the commonly accepted value for P_r is 7.0 (Fischer *et al.*, 1979). Coupled with the modified A_z algorithm, the D_z changes significantly improved modelled western and central basin temperature time series (Figs. 4c and 4d).

Results

Water Level

At both Toledo and Buffalo the modelled water levels follow the lowest mode period of 14 h (0.07 cph) very well with respect to wavelength, phase and amplitude (Fig. 6c and Table 3). Storm surges up to one meter in height are frequent in the observed and modelled time series (e.g. days = 147, 176). The modified CE-QUAL-W2 simulates these large surface level changes extremely well (Figs. 6a and 6c).

Water level frequency spectra were estimated by dividing the time series into segments 256 points in length, using a 256-point Blackman window and overlapping adjacent segments by 128 points. Frequencies of the lowest 3 natural surface seiche modes (0.07, 0.11 and 0.17 cph) are clearly evident in both the modelled and observed energy spectra from Toledo (Fig. 6d). Low frequency high-energy peaks can also be seen in both the modelled and observed water level

spectra at periods of 100 h (0.01 cph) and 24 h (0.042 cph). These same frequencies are evident in the frequency spectrum of the longitudinal wind component (Fig. 6b). Platzman and Rao (1964) concluded that the diurnal (0.042 cph) peak in the water level spectra was due to the diurnal component in the atmospheric forcing on the lake; while Hamblin (1987) and Boyce and Chiocchio (1987) found their 100 h (0.01 cph) peak to be a direct result of a dominance of storm events with time-scales greater than 1 d.

CE-QUAL-W2's omission of a lunar tidal component was found to be inconsequential, as no semidiurnal peak indicating direct gravitational tidal action is evident in the observed water level spectra. Platzman (1966) also concluded that the semidiurnal astronomical tide is negligible in Lake Erie.

Currents

Comparison of modelled and observed longitudinal currents at depths of 3.4 and 8 m at the western basin station (W_2) showed reasonable agreement both in phase and amplitude (Fig. 7), however the agreement at 8.0 m is not as good. Observed and modelled energy spectra for current velocities (Figs. 7b and 7d) both exhibit Lake Erie's lowest three natural barotropic frequencies (0.07, 0.11 and 0.17 cph). The spectral peaks are better defined in the modelled spectra as the modelled time series is of significantly greater length. Wind-forced diurnal and 0.01 cph storm frequency peaks (Fig. 6b) may be seen in both modelled and observed longitudinal current energy spectra.

The seasonal mean flow is typically positive (from west to east) in both the western and central basins (Table 4), corresponding to the west-east direction of the lake's natural hydraulic flow. Modelled and observed time series have similar means and standard deviations at both 3.4 and 8 m depths (Table 4). However, direct comparison of central basin longitudinal current time

series is difficult because the observed 0.056-cph inertial currents, which result from Coriolis effects on basin-scale Poincaré waves (Mortimer, 1974), are quite strong in the central basin epilimnion but are removed through lateral averaging of CE-QUAL-W2's governing equations as is evident in (Fig 5d). In the central basin at depths of 3m and 11 m the observed longitudinal current seasonally averaged standard deviation (Table 4) is nearly twice the modelled current standard deviation. This difference is indicative of the strength of the observed current's inertial oscillation (Fig. 5a).

Both the modelled and observed central basin current time series at 3, 11 and 24 m depths have spectral peaks at periods of 100 h (0.01 cph), 24 h (0.042 cph), 14 h (0.07 cph) and 6 h (0.17 cph) (Fig. 5d,e,f). The 14 and 6-h currents correspond to the first and third modes of the surface gravitational seiches. The 9-h second mode (0.11 cph) is only predicted at a depth of 24 m. At 24 m where the observed time series (measured 1 m above the bed) is relatively quiescent, the model predicts 1.5 orders of magnitude more spectral energy at 0.01 and 0.07 cph than is observed (Fig. 5f). The excess energy at low frequencies is caused by a large amplitude internal seiche that is predicted by the model but not observed in the field data. In large lakes, such as Lake Erie, where Coriolis effects are significant, basin scale oscillations below the inertial frequency (0.056 cph) are classified as Kelvin waves and due to rotation have little influence beyond 20 km offshore (Mortimer, 1974). Nevertheless, overall the modelled current velocities agree well with the 1994 field observations, and those of Boyce and Chiocchio (1987) from 1980, with the exception that the spectral energies of the modelled 0.01 cph frequency near the bed are higher.

Temperatures

The vertical and longitudinal variation in water temperature predicted by the model for the western basin (i.e. station W1) are very similar to those found in the observed data for this location (Fig. 4c & 8). The water column is fully mixed until late June when stratification occurs near day 173 (June 23). The model lags behind the observations by approximately three days (e.g. the model predicts the occurrence of the 15°C isotherm on day 152 (June 1), yet it was observed on day 149). The mean absolute error between the modelled and observed western basin temperature time series is less than 0.6°C (Table 5).

In both the modelled and observed results for central basin station C (Fig. 1), the degree of stratification increases through June culminating with a firmly established thermocline at a depth of approximately 20 m by day 196 (July 15) (Fig. 9). Previous field measurements have shown that the thermocline is usually firmly established by the middle of July at a depth of 15 m (Schertzer *et al.*, 1987). This distinct thermocline persists through the end of the simulation (day 269). In the epilimnion, the water temperature increases from Julian day 130 through 215. Detailed examination of the surface temperature time series shows that the amplitudes of the daytime heating peaks are under-predicted when the magnitude of observed daytime heating is very large (e.g. days 158,170, and 195) but these high frequency isotherm fluctuations are not reproduced by the model (Fig. 9). The omission of this heat input, which cycles with the incident short-wave radiation results in reduced vertical mixing by penetrative convection and a slight under-prediction of epilimnetic temperatures. Nevertheless, temperatures are well modelled at all depths, with the mean error ranging between 1.41 and 1.82°C. The mean error, as expected, is greater in the central basin than in the well-mixed western basin because simulating temperatures within a thermally stratified water column is inherently more difficult.

The formation and location of the thermocline in the eastern basin station (E) are well simulated by the model (Fig. 10); however, the observed thermocline has a steeper temperature gradient. Thickening of the metalimnion likely results from both the increased A_z values and artificially from numerical diffusion (Hodges *et al.*, 1999). In both the central and eastern basins the model correctly simulates the sharpening and deepening of the thermocline through August and September. However, as in the central basin the high frequency diurnal isotherm oscillations evident in the observed epilimnion data are not reproduced by the model. The modelled isotherms exhibit a strong 4-5 day (0.01 cph) low frequency oscillation with an amplitude of approximately 10 m. Note, once again, that this 0.01 cph frequency is the dominant frequency in both the surface wind forcing (Fig. 6b) and the excessively strong central basin 24 m current (Figs. 5d and 5f). Within the epilimnion and metalimnion the mean absolute error between the modelled and observed temperatures ranges from 1.129 to 1.729°C (Table 5). In the deep, quiescent hypolimnion, the temperature remains near 4°C throughout the season in both the observed and modelled results with a maximum mean error of 0.657°C.

Thermocline deepening events are correctly simulated as step-like temperature increases observed near days 148, 160 and 176 (Figs. 4c, 4d). These events correspond to strong surface wind forcing (Fig. 6-a), resultant water level storm surges (Fig. 6-c), increased vertical mixing in the epilimnion and a deepening of the modelled and observed mixed layer near days 148, 160, and 175 (Figs. 8 and 9). This is consistent with Schertzer *et al.*'s (1987) observations that mixed layer deepening in the central basin was primarily associated with strong wind events.

Dissolved Oxygen

Using default kinetic rate constants from Cole and Buchak (1995) (Table 6), CE-QUAL-W2 was used to simulate Lake Erie's algal/nutrient/dissolved oxygen dynamics. Dissolved

oxygen profiles were sampled during three summer cruises in 1994 at a series of stations corresponding to various segments in the model (Fig. 11a). The model reproduces the general magnitudes and trends of the observed dissolved oxygen profiles (Fig. 11b-d). For example, on 15 June (day 166), prior to stratification, the lake-wide water column dissolved oxygen is relatively constant with depth with the exception of the deep eastern basin (Fig. 11b). On 20 July (day 201), stratification has created a thin hypolimnion at the interface of the western and central basins, preventing vertical transport of oxygenated surface water thus allowing the sediment oxygen demand to lower the hypolimnetic dissolved oxygen to below 5 mg/l (Fig. 11c, segments S43, S56, S64 and S74). West of the central/eastern basin interface (S145) the dissolved oxygen is modelled to increase by 5 mg/l through the hypolimnion. This results from the movement of cold, oxygen-rich eastern basin hypolimnetic water. In late August – early September (e.g., day 243), the oxygen-depleted region has expanded to the central basin (Fig. 11d, segments S97 and S106), following the sharpening and deepening of the thermocline. These results agree with Charlton's (1980) findings and those of Lam et al.'s (1983) that the degree of meteorologically induced stratification, as opposed to nutrient loading, was found to strongly influence the presence of central basin anoxia.

Discussion

CE-QUAL-W2's eddy viscosity turbulence model, developed for narrow, hydraulically driven lakes and reservoirs, was found to be inappropriate for large, wind-driven lakes as Lake Erie (Figs. 3 and 4). However, increasing vertical mixing coefficients to above normally accepted values corrected for processes not contained within the model's framework. This modification reduced the modelled currents in the epilimnion and the fully mixed western basin

to the same order of magnitude as those observed in the field and brought modelled temperatures to within 3°C of observed. Despite the adoption of abnormally high mixing coefficients the model still predicted, large-amplitude, low-frequency longitudinal current oscillations in the stratified central basin hypolimnion and in the eastern basin.

Bartish (1987) observed that eastern/central basin hypolimnetic transport was governed by wind forcing, local bathymetry, and the characteristics of stratification. Bartish (1987) and Saylor and Miller (1987) found net hypolimnetic transport at the junction of the central and eastern basins to be westward (see Table 4). The principal driving force behind this flow results from southwest winds forcing central basin surface water into the eastern basin. Eastern basin hypolimnetic return flow is then funneled westward, constricted by the thermocline, into the central basin. At the onset of stratification, the shallow thermocline in the eastern and central basin is above the depth of the crest of the Pennsylvania Ridge (Fig. 1) and hypolimnetic exchange flow is unhindered. As the thermocline deepens through the summer, the hypolimnia, and later the metalimnia, are separated by the Pennsylvania Ridge (Bartish, 1987). This limits flow to the Pennsylvania Channel where up to 80-100% of the hypolimnetic flow can occur (Chiocchio, 1981). Continued deepening of the thermocline in early autumn leads to an isothermal central basin, while the eastern basin thermocline drops below the level of the Pennsylvania Channel (Bartish, 1987) thus blocking exchange flow. Major exchange events result from extreme meteorological forcing (Bartish, 1987). Normal exchange flow was seen to periodically fluctuate through the channel at periods of 50-150 h (Chiocchio, 1981) and 100 h (0.01 cph) by Boyce *et al.* (1980). These observations are in agreement with the typical storm cycle (Bartish, 1987; Fig. 6b) and the frequency of the large amplitude central basin currents (Fig. 5f).

Bartish (1987) suggests that the Pennsylvania Current is a result of internal seiche forcing in the deep stratified eastern basin. The model predicts seiches with average frequencies of 0.01 cph (Fig. 10a), similar to those observed by Bartish (1987) in Lake Erie's eastern basin in 1977. The theoretical period of the longitudinal internal seiche in the eastern basin was estimated to be approximately 103 h (0.0097 cph). The proximity of the periods of environmental forcing and natural oscillation likely results in a resonantly amplified forced oscillation (Mortimer, 1974).

We modified the A_z algorithm to further increase the vertical diffusion of momentum, in an attempt to increase damping of the simulated hypolimnetic central basin currents (Boegman, 1999). We increased the surface A_z maximum value by approximately two orders of magnitude to (~ 1.0 m^2/s) and the bed A_z by one order of magnitude to (~ 0.5 – 1.0 m^2/s), and found A_z had reached an upper limit of influence because these larger mixing coefficients resulted in a negligible reduction in hypolimnetic current velocity. Increased damping of internal waves was also attempted by the inclusion of sidewall friction (Stacey *et al.*, 1995), again with negligible effect.

Lateral averaging of basin depth results in oversimplification of the complex bathymetry in the Pennsylvania Ridge and Channel region and could cause the model to predict excessive exchange between the central and eastern basins. Sensitivity analysis of the blocking effect of the Pennsylvania Ridge, however, showed that increasing the height of the ridge had a negligible effect on central basin hypolimnetic currents.

Removing the Richardson number dependence of A_z in the thermocline region was found to reduce central basin hypolimnetic currents. However, this also prevented stratification because it allowed for enhanced vertical mixing, and thus a distinct thermocline was not predicted in either the central or eastern basins.

It is unlikely that model results could be further improved through the use of the K- ε turbulence model (K = turbulent kinetic energy and ε = turbulence dissipation rate) that, unlike the empirical eddy coefficient turbulence model used here, eliminates the need to empirically prescribe the turbulent length scale (Johnson, 1998). The magnitudes of vertical mixing employed herein are much larger than those given by the K- ε turbulence model. In an attempt to directly account for the dissipation of energy in the internal wave field, Ivey *et al.*, (1998) have, proposed a dissipation term that specifies the energy loss in the benthic boundary layer assuming that all energy of an incident internal wave is absorbed at the boundary when the bed slope is critical.

An important aspect of this study is the determination of the effects of lateral averaging for Lake Erie. Although Lake Erie has a 6:1 length-to-width aspect ratio it has a maximum width greater than 100 km, many times the internal Rossby radius of deformation (~ 5 km). That is, at length scales greater than ~5 km in Lake Erie the effects of the earth's rotation become important. This being the case, momentum transfer by Coriolis forces, from longitudinal to transverse, could be acting to reduce longitudinal basin-scale seiche strength by directing momentum laterally, away from the lake's longitudinal axis. A simple analytical model for the current excited by a sudden increase in wind shear acting on the epilimnion, gives the longitudinal current velocity in the inertial (non-rotating) frame, U_I, as the product of the wind stress, w, times the elapsed time, t, divided by the product of water density, ρ, and epilimnion thickness, h:

$$U_I = \frac{wt}{\rho h} \tag{7}$$

The longitudinal current in the rotational frame, U_R, is given by,

$$U_R = \frac{w}{\rho h}\frac{\sin(ft)}{f} \tag{8}$$

where f is the Coriolis parameter for Lake Erie, $f = 9.77 \times 10^{-5}\ s^{-1}$ (Gill, 1982). For a short time, the two flows are close in speed and direction, but after one-quarter of an inertial period (~ 4.5 h for Lake Erie) the longitudinal current in the rotational flow vanishes and after 9 h it opposes the wind. This simple analysis suggests that the reduction of longitudinal momentum is compensated for in the 2-D model case by augmented values of vertical eddy viscosity.

CE-QUAL-W2 is a laterally averaged model and as such cannot account for the effects of rotation, nevertheless, when vertical mixing rates were adjusted as described earlier, temperatures and dissolved oxygen levels were accurately modelled at lake centre-line stations. Thus, we found that CE-QUAL-W2 is capable of accurately predicting the longitudinal gradients in temperature and water quality parameters measured by Charlton (1994). Despite its inability to model inertial (Coriolis) currents because of the lateral averaging, temperature and dissolved oxygen predictions were in excellent agreement with observed values even in the vast central basin. This is perhaps because the central basin is relatively homogeneous horizontally (Ivey and Patterson, 1984).

Conclusions

Modifications to CE-QUAL-W2's vertical mixing algorithm were required to suppress excessive low frequency wind forced oscillations in the western basin and central basin epilimnion. In these regions, once the vertical mixing routine was adjusted, longitudinal currents were modelled qualitatively with the possible exception of near-bed currents in the central basin. The model accurately predicted water levels, dissolved oxygen profiles and the thermal structure.

These results support the further extension of the model to include the effects of zebra mussels and zooplankton under a regimen of varying nutrient inputs and meteorological forcing.

Acknowledgements

The assistance of T. Cole in modifying the CE-QUAL-W2 source code and providing advice is gratefully acknowledged. The authors are grateful to F.M. Boyce who was responsible for the collection of moored meteorological, temperature and current meter data in the central and eastern basins. This project was funded by the Ohio Sea Grant College Program Grant NA86RG0053 (Project R/EM-20) to D.A.C., and by the Ohio State University and the University of Toronto.

Numerous agencies and individuals provided flow and nutrient loading data. The United States Geological Survey provided the Maumee and Sandusky River inflows and the Niagara River outflow. NOAA provided the Detroit River inflow and over lake precipitation measurements. Environment Canada provided Grand River (Ontario) inflow data. The Ontario Ministry of the Environment provided Detroit and Grand River temperatures and nutrient loadings. Peter Richards at Heidelberg College, Tiffin, Ohio, provided Maumee and Sandusky River temperatures and nutrient loadings. The United States Environmental Protection Agency provided the Welland Canal outflow and the flows, temperatures and nutrient loadings from the Erie (Pennsylvania) and Toledo, Cleveland Easterly and Cleveland Westerly (Ohio) wastewater treatment plants.

References

Adams, W.R., E.L. Thackston and R.E. Speece. 1997. Modeling CSO impacts from Nashville using EPA's demonstration approach. J. Envir. Engr. **123**: 126-133.

Arnott, D.L. and Vanni, M.J. 1996. Nitrogen and phosphorus recycling by the zebra mussel (Dreissena polymorpha) in the western basin of Lake Erie. Can. J. Fish. Aquat. Sci., 53:646-659.

Bartish, T. 1987. A review of the exchange processes among the three basins of Lake Erie. J. Great Lakes Res. **13**: 607-618.

Berkman, P.A., M.A. Haltuch, E. Tichich, D.W. Garton, G.W. Kennedy, J.E. Gannon, S.D. Mackey, J.A. Fuller and D.L. Liebenthal. 1998. Invading mussel beds in Lake Erie. Nature. **393**: 27-28.

Boegman, L. 1999. Application of a two-dimensional hydrodynamic and water quality model to Lake Erie. M.A.Sc. thesis, Department of Mechanical and Industrial Engineering, University of Toronto, Ont., Canada.

Boyce, F.M. and F. Chiocchio. 1987. Water movements at a mid-central basin site: time and space scales, relation to wind and internal pressure gradients. J. Great Lakes Res. **13**: 530-541.

Boyce, F.M., F. Chiocchio, B. Eid, F. Penicka and F. Rosa. 1980. Hypolimnion flow between the central and eastern basins of Lake Erie during 1977. J. Great Lakes Res. **6**: 290-306.

Charlton, M.N. 1980. Hypolimnion oxygen consumption in lakes: discussion of productivity and morphometry effects. Can. J. Fish. Aquat. Sci., 37:1531-1539.

Charlton, M.N. 1994. The case for research on the effects of zebra mussels in Lake Erie: Visualization of information from August and September 1993. J. Biological Systems. **2**: 467-480.

Chiocchio, F. 1981. Lake Erie hypolimnion and mesolimnion flow exchange between central and eastern basins during 1978. National Water Research Institute, Canada Centre for Inland Waters, Internal Report, APSD 009, Burlington, Ont.

Cole, T.M. and E.M. Buchak. 1995. CE-QUAL-W2: A two-dimensional, laterally averaged, hydrodynamic and water quality model, version 2.0: User manual. Instruction Report EL-95-1, US Army Engineer Waterways Experiment Station, Vicksburg, MS.

Fischer, H.B., E.J. List, R.C.Y. Koh, J. Imberger, and N.H. Brooks. 1979. Mixing in Inland and Coastal Waters. Academic Press, New York, N.Y. pp.483.

Fréchette, M., C.A. Butman, and W.R. Geyer. 1989. The importance of boundary-layer flows in supplying phytoplankton to the benthic suspension feeder, *Mytilus edulis* L. Limnol. Oceanogr., **34**: 19-36.

Gill A.E. 1982. Atmosphere-Ocean Dynamics. Academic Press, New York, NY.

Hamblin, P. F. 1987. Meteorological forcing and water level fluctuations on Lake Erie. J. Great Lakes Res. **13**: 436-453.

Hodges, B.R., J. Imberger, A. Saggio, and K.B. Winters. 1999. Modeling basin scale internal waves in a stratified lake. CWR manuscript ED 1452-BH, Department of Environmental Engineering, University of Western Australia, Nedlands WA, Australia (submitted to Limnol. Oceanogr.).

Holland, R. 1993. Changes in planktonic diatoms and water transparency in Hatchery Bay, Bass Island area, western Lake Erie since the establishment of the zebra mussel. J. Great Lakes Res. **19**: 617-624.

Ivey, G. N., J. Imberger, and J. R. Koseff. 1998. Buoyancy fluxes in a stratified fluid. *In* Physical Processes in Lakes and Oceans. *Edited by* J. Imberger. American Geophysical Union, Washington, D.C. pp. 377-388.

Ivey, G.N. and J.C. Patterson. 1984. A model of the vertical mixing in Lake Erie in summer. Limnol. Oceanogr. **29**: 553-563.

Johnson, R.W. 1998. The handbook of fluid dynamics. CRC Press, Boca Raton, FL.

Kuan, C. 1995. Qualitative skill assessment of the Princeton coastal ocean circulation model for Lake Erie. Ph.D. thesis, Department of Civil Engineering, The Ohio State University, Columbus, OH.

Lam, D.C.L., W.M. Schertzer and A.S. Fraser. 1983. Simulation of Lake Erie water quality responses to loading and weather variations. The National Water Research Institute, Inland Waters Directorate, Canada Centre for Inland Waters, Burlington, Ont. Scientific Series No. 134.

Leach, J.H. 1993. Impacts of the zebra mussel on water quality and fish spawning reefs in western Lake Erie. *In* Zebra Mussels: Biology, Impacts and Control. *Edited by* T.F. Nalepa and D.W. Schloesser. 381-398.

Madenjian, C.P. 1995. Removal of algae by the zebra mussel (*Dreissena polymorpha*) population in western Lake Erie- a bioenergetics approach. Can. J. Fish. Aquat. Sci., 52: 381-390.

Martin, J.L. 1988. Application of two-dimensional water quality model. J. Envir. Engr. **114**: 317-336.

McCune, K.C. 1998. Temperature gradient microprofiling in the central basin of Lake Erie: A study of vertical turbulent process. M.Sc. thesis, Department of Civil Engineering, The Ohio State University, Columbus, OH.

Mortimer, C.H. 1974. Lake hydrodynamics. Mitt. Intenat. Verein. Limnol. **20**: 124-197.

Nicholls, K.H. and G.J. Hopkins. 1993. Recent changes in Lake Erie (north shore) phytoplankton: cumulative impacts of phosphorus loading reductions and the zebra mussel introduction. J. Great Lakes Res. **19**: 637-647.

Nicholls, K.H., D.W. Standen, G.J. Hopkins and E.C. Carney. 1977. Declines in near-shore phytoplankton of Lake Erie's western basin since 1971. J. Great Lakes Res. **3**: 72-78.

Platzman, G.W. 1966. The daily variation of water level on Lake Erie. J. Geophys. Res. **71**: 2472-2483.

Platzman, G.W. and D.B. Rao. 1964. Spectra of Lake Erie water levels. J. Geophys. Res. **60**: 2525-2535.

Saggio, A. and J. Imberger. 1998. Internal weather in a stratified lake. Limnol. Oceanogr. **43**: 1780-1795. Saylor, J.H. and G.S. Miller. 1987. Studies of large-scale currents in Lake Erie,1979-80. J. Great Lakes Res. **13**: 487-514.

Schertzer, W.M. 1987. Heat balance and heat storage estimates for Lake Erie, 1967 to 1982. J. Great Lakes Res. **13**: 454-467.

Schertzer, W.M. and P.F. Hamblin. 2000. Lake Erie thermal structure: Variability, trends and potential changes. *In*: Lake Erie at the Millenium. *Edited by* J.H. Ciborowski. University of Windsor, April 26-28, 1999. Accepted for publication.

Schertzer, W.M., J.H. Saylor, F.M. Boyce, D.G. Robertson and F. Rosa. 1987. Seasonal thermal cycle of Lake Erie. J. Great Lakes Res. **13**: 468-486.

Stacey, M.W., S. Pond and Z.P. Nowak. 1995. A numerical model of the circulation in Knight Inlet, British Columbia, Canada. J. Phys. Oceanogr. **25**: 1037-1062.

T.V.A. 1972. Heat and mass transfer between a water surface and the atmosphere. Tennessee Valley Authority Rep. No. 0-6803, Knoxville, TN.

Input	Maximum	Minimum	Mean
Air Temperature (°C)	30.3	4.6	19.4
Wind Speed (m/s)	16.2	0	4.5
Detroit River Flow (m^3/s)	6051	5302	5709
Detroit River Temp. (°C)	24.0	12.0	20.6
Niagara River Flow (m^3/s)	6824	5720	6284

Table 1: Variation in meteorological and inflow/outflow data for Lake Erie from 20 May to 13 September 1994.

Zone	Original A_z routine developed for hydraulically-driven lakes	Modified A_z routine developed for wind-driven Lake Erie
Epilimnion	$A_z = 10^{-4}$ m/s^2. Surface currents 3-10% of surface wind speed.	Increased A_z by 2 orders of magnitude to $A_z = 10^{-2}$ m/s^2 to reduce surface currents to 2–3% of surface wind speed.
Metalimnion	A_z reduction as a function of local R_i prevents mixing across thermocline.	Placed limit on R_i reduction and increased A_z to account for metalimnetic dissipation.
Hypolimnion	A_z _ 0 at bed. Very strong internal seiche developed affecting inter-basin exchange flow.	Increased A_z by 4 orders of magnitude to $0.05 = A_z = 0.1$ m/s^2 to increase benthic dissipation.

Table 2: Summary of vertical eddy viscosity modifications to the original CE-QUAL-W2 source code.

Location	Mean (m)	Standard Deviation (m)
Buffalo observed	174.5141	0.1041
Buffalo modelled	174.5099	0.0909
Toledo observed	174.5223	0.1167
Toledo modelled	174.4813	0.0985

Table 3: Comparison of observed and modelled water levels at the Buffalo and Toledo field sites.

Station	Mean (m/s)	Standard Deviation (m/s)
W_2 3.4 m observed	0.019	0.041
W_2 3.4 m modelled	0.012	0.027
W_2 8.0 m observed	0.010	0.028
W_2 8.0 m modelled	0.009	0.030
C 3.0 m observed	-.0090	0.0694
C 3.0 m modelled	0.0232	0.0371
C 11 m observed	0.0105	0.0499
C 11 m modelled	0.0017	0.0271
C 24 m observed	0.0197	0.0141
C 24 m modelled	-0.0088	0.0524

Table 4: Comparison of modelled and observed seasonal mean longitudinal current velocity variation with depth at western basin station W_2 and central basin station C.

Station W_1		Station C		Station E	
Depth (m)	Mean Error (°C)	Depth (m)	Mean Error (°C)	Depth (m)	Mean Error (°C)
0.0	0.528	0.0	1.451	0.0	1.172
2.0	0.355	2.0	1.818	2.0	1.129
5.0	0.564	5.0	1.588	10.0	1.513
9.4	0.586	8.0	1.433	20.0	1.729
-	-	11.0	1.418	35.0	0.657
-	-	14.0	1.518	50.0	0.310
-	-	17.0	1.771	61.0	0.298
-	-	24.0	1.413	-	-

Table 5: Mean absolute error of modelled temperature for the western basin (station W_1), central basin (station C) and eastern basin (station E) time series.

Mean absolute error = $(\sum_{i=1}^{n} |(\text{observed temperature})_i - (\text{modelled temperature})_i|) / n$

Kinetic Parameter	Suggested Range (Cole and Buchak 1995)	Value Used
Algal growth rate	1.1-2.0 day^{-1}	1.1 day^{-1}
Algal mortality rate	0.01-0.1 day^{-1}	0.1 day^{-1}
Algal excretion rate	0.01-0.04 day^{-1}	0.04 day^{-1}
Algal dark respiration rate	0.02-0.04 day^{-1}	0.04 day^{-1}
Algal settling rate	0.1-0.14 m/day	0.1 m/day
Labile dissolved organic material decay rate	0.12 day^{-1}	0.12 day^{-1}
Detritus decay rate	0.06-0.08 day^{-1}	0.08 day^{-1}
Nitrate decay rate	0.05-0.15 day^{-1}	0.05 day^{-1}
Ammonium decay rate (oxidation to nitrate)	0.12 day^{-1}	0.12 day^{-1}
Sediment oxygen demand	0.1-1.0 g O_2 m^2/day	0.35 O_2 m^2/day
Chézy bed roughness coefficients		
Western Basin	70 $m^{1/2}/s$	90 $m^{1/2}/s$
Central basin	70 $m^{1/2}/s$	90 $m^{1/2}/s$
Eastern basin	70 $m^{1/2}/s$	30 $m^{1/2}/s$
Turbulent Prandtl numbers		
Western basin	7.0	2.0
Central basin	7.0	2.0
Eastern basin	7.0	7.0

Table 6: Physical parameters and kinetic rate constants used in the application of CE-QUAL-W2 to Lake Erie.

Figures Captions

Figure 1: Lake Erie bathymetric plan view. Note major geological features and 1994 monitoring buoy locations as marked.

Figure 2: CE-QUAL-W2 solution plane (longitudinal cross-section) showing width contours, contour interval is 25 km.

Figure 3: Time series of observed * (·····) and modeled (———) longitudinal current velocities (Panels a, b, c) and energy spectra (Panels d, e, and f) for the original A_z algorithm at three depths in central Lake Erie at Station C. Time scales are in calendar days.

Figure 4: Time series of observed (·····) and modeled (———) temperature variations for the original A_z algorithm at 9.4 m in the western basin (Panel a) and at 14 m in the central basin (Panel b), and the modified A_z algorithm in the western basin (Panel c) and the central basin (Panel d). Time scales are in calendar days.

Figure 5: Time series of observed (·····) and modeled (———) longitudinal current velocities (Panels a, b, c) and energy spectra (Panels d, e, and f) for the modified A_z algorithm at three depths in central Lake Erie at Station C. Time scales are in calendar days.

Figure 6: Time series comparing the central basin longitudinal wind speed (Panel a) and the observed (·····) and modeled (———) Toledo water levels (Panel b) and their respective energy spectra (Panels c and d). Time scales are in calendar days.

Figure 7: Time series comparing the observed * (·····) and modeled (——) longitudinal currents in the western basin at 3.4 m (Panel a) and 8.0 m (Panel b), and their respective energy spectra (Panels c and d). Time scales are in calendar days.

Figure 8: Time series comparing the modeled (Panel a) and observed (Panel b) vertical temperature distribution in western Lake Erie (Station W1). Isotherm interval = 2.5°C. Time scales are in calendar days.

Figure 9: Time series comparing the correspondence between the modeled (Panel a) and observed (Panel b) temperature distribution with depth in central Lake Erie (Station C). Isotherm interval = 2.5°C. Time scales are in calendar days.

Figure 10: Time series comparing the correspondence between the modeled (Panel a) and observed (Panel b) temperature distribution with depth in eastern Lake Erie (Station E). Isotherm interval = 2.5°C. Time scales are in calendar days.

Figure 11a: Longitudinal locations of individual oxygen profiles (S = segment).

Figure 11b: Comparisons of vertical profiles of dissolved oxygen concentrations at segments 23 – 193 for 13-17 June 1994, , observed (·····) and modelled (——) .

Figure 11c: Comparisons of vertical profiles of dissolved oxygen concentrations at segments 23 – 193 for 18-22 July 1994, observed (·····)and modelled (——).

Figure 11d: Comparisons of vertical profiles of dissolved oxygen concentrations at segments 23 – 193 for 29 August – 2 September 1994, observed (·····)and modelled (——).

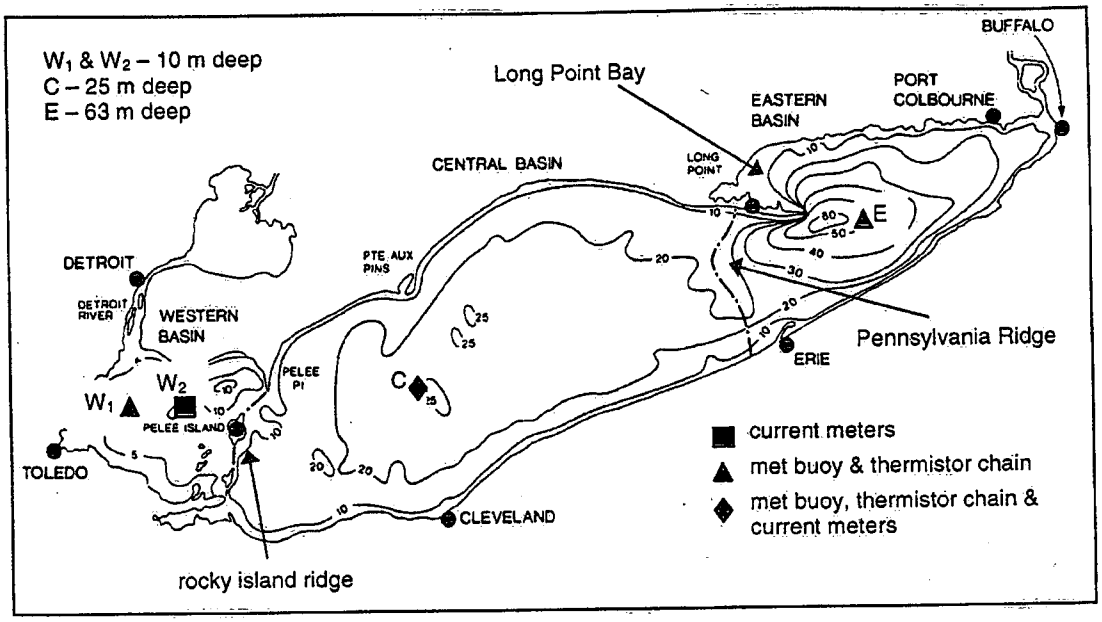

Figure 1: Boegman, Loewen, Hamblin, Culver and Charlton

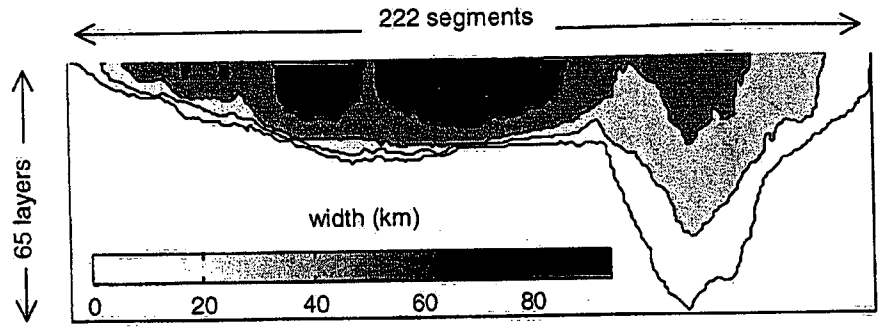

Figure 2: Boegman, Loewen, Hamblin, Culver and Charlton

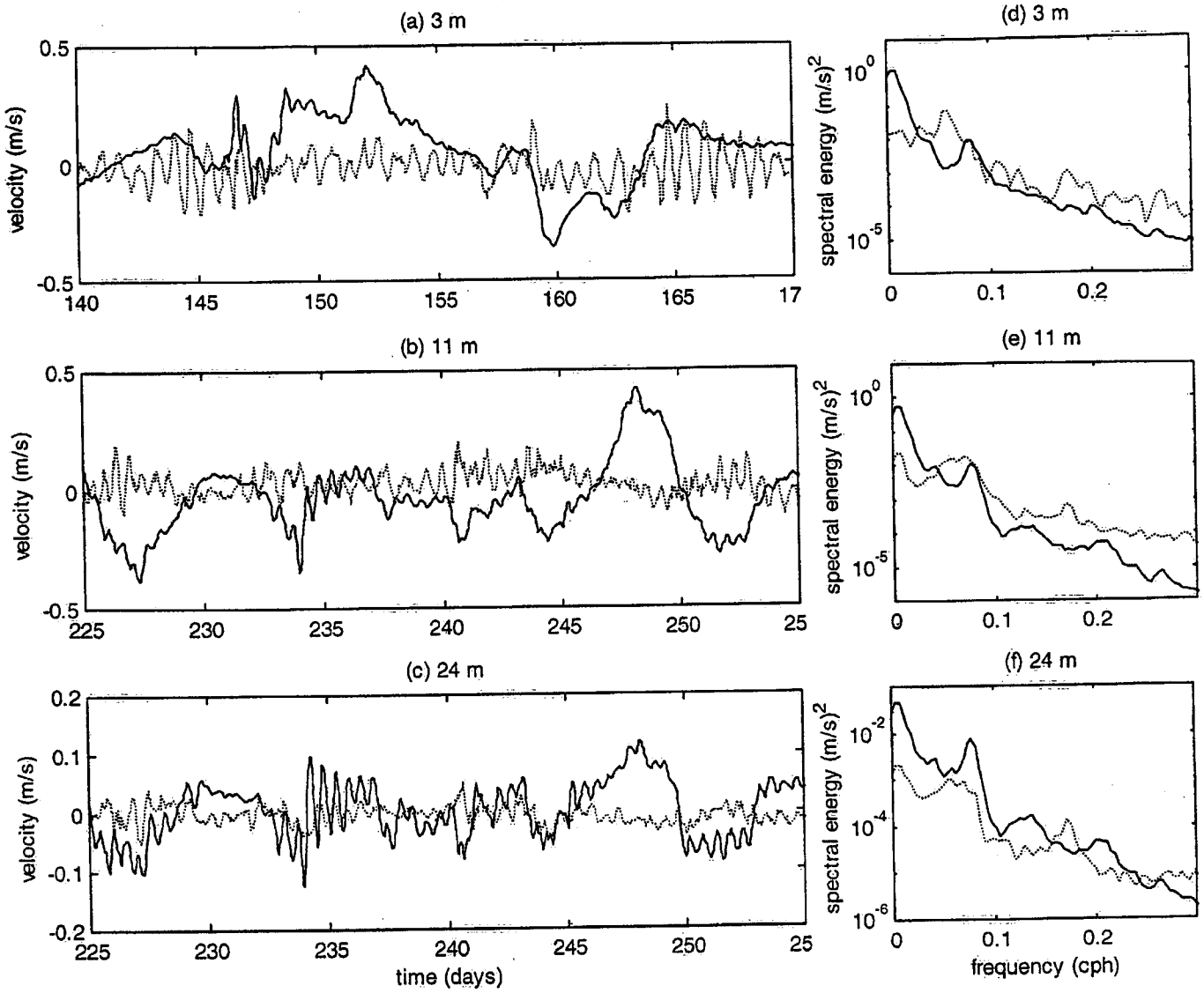

Figure 3: Boegman, Loewen, Hamblin, Culver and Charlton

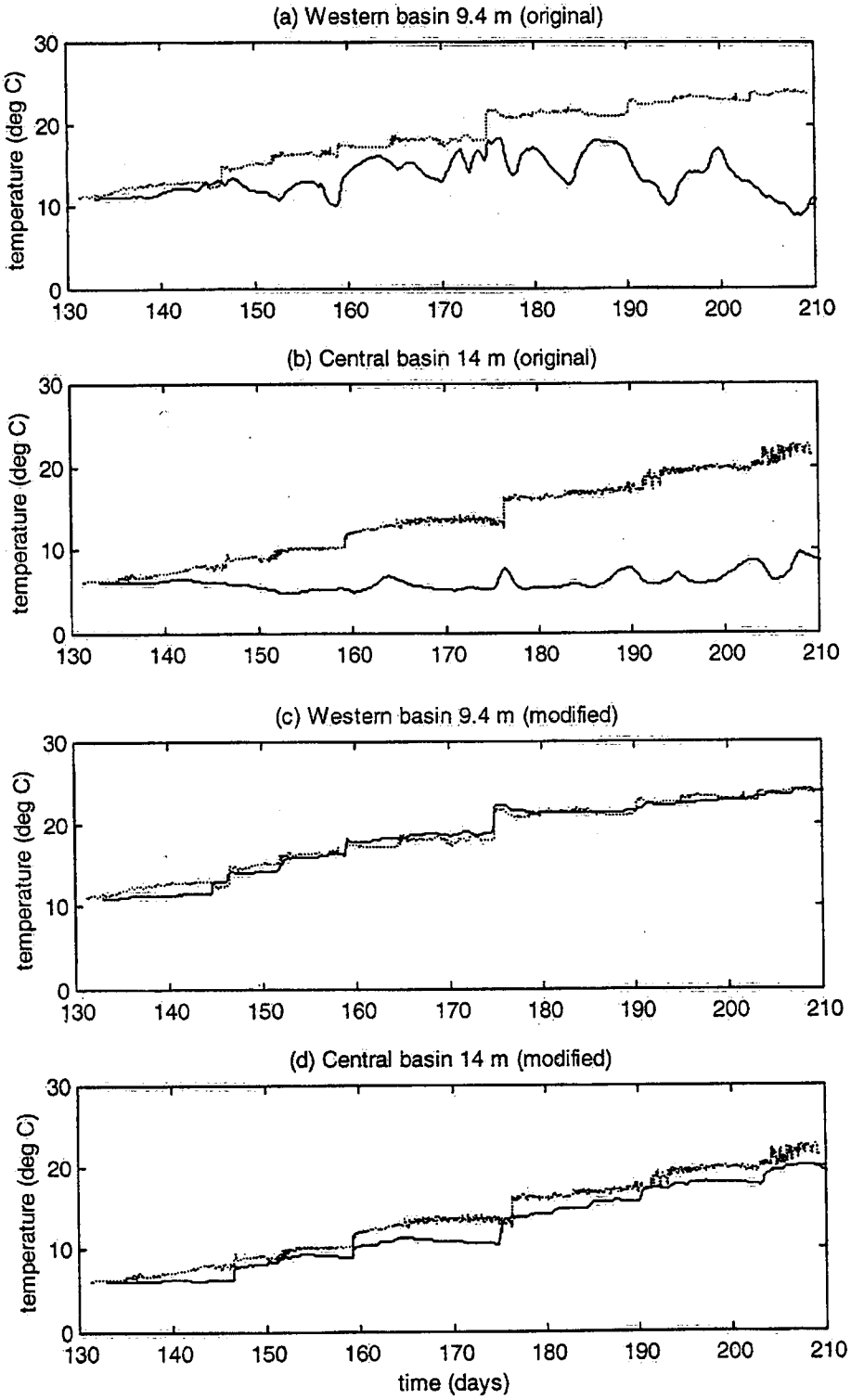

Figure 4: Boegman Loewen, Hamblin, Culver and Charlton

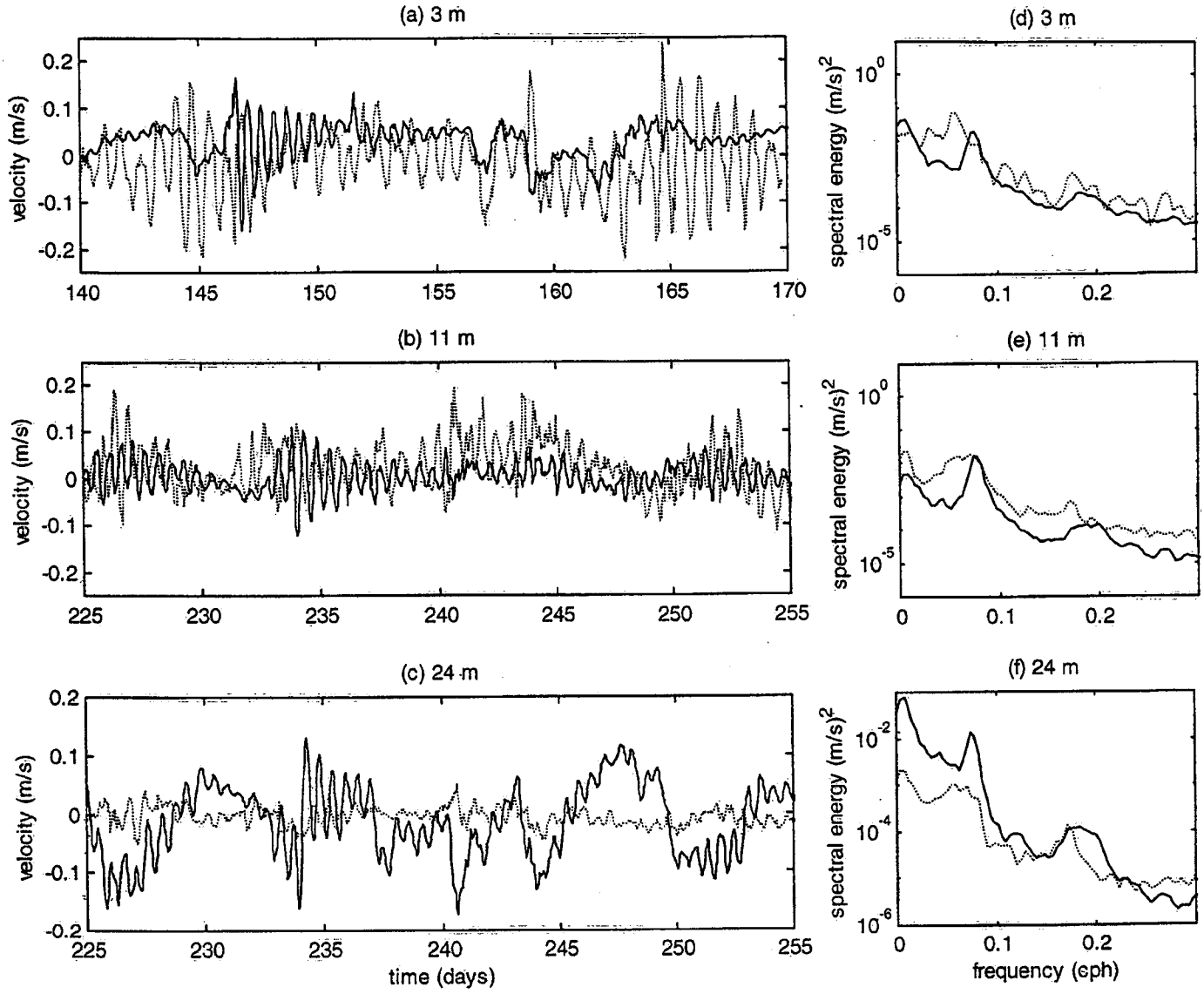

Figure 5: Boegman, Loewen, Hamblin, Culver and Charlton

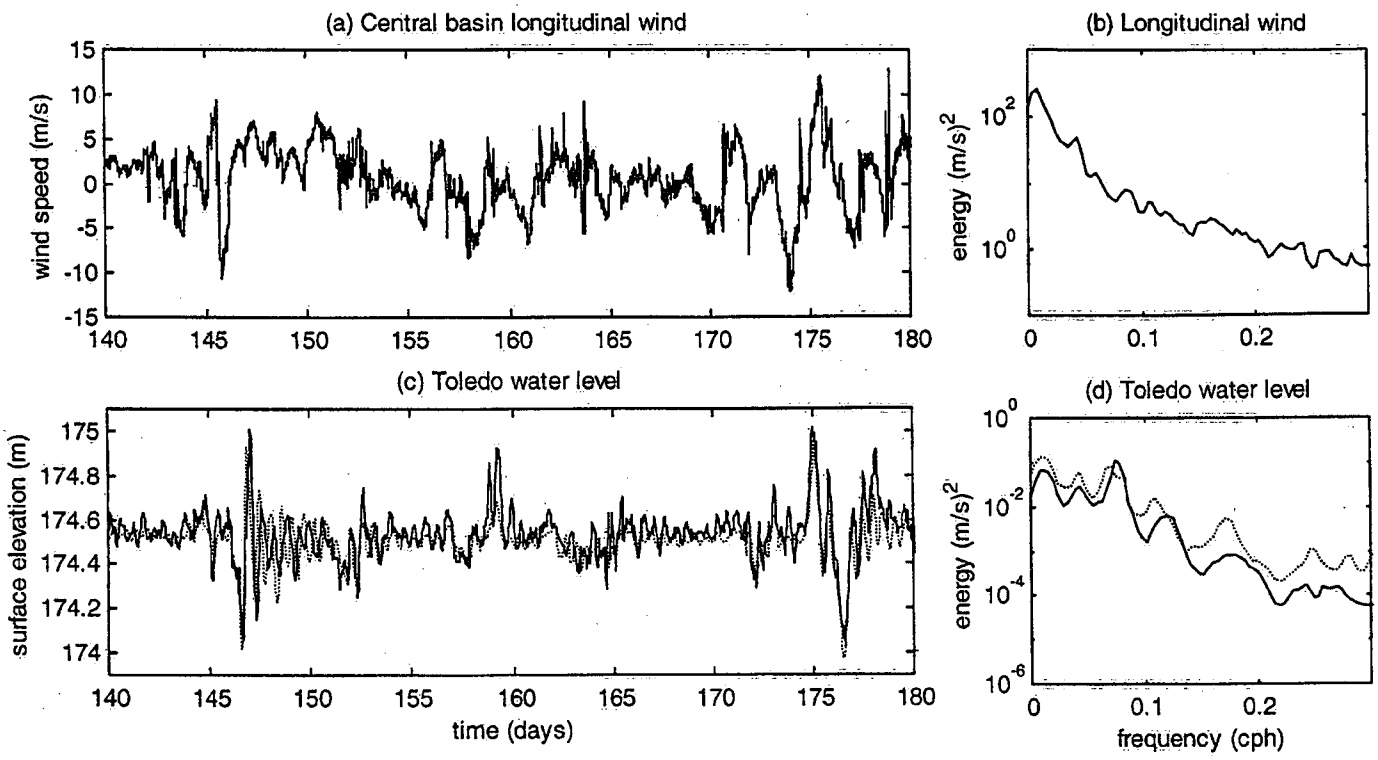

Figure 6: Boegman, Loewen, Hamblin, Culver and Charlton

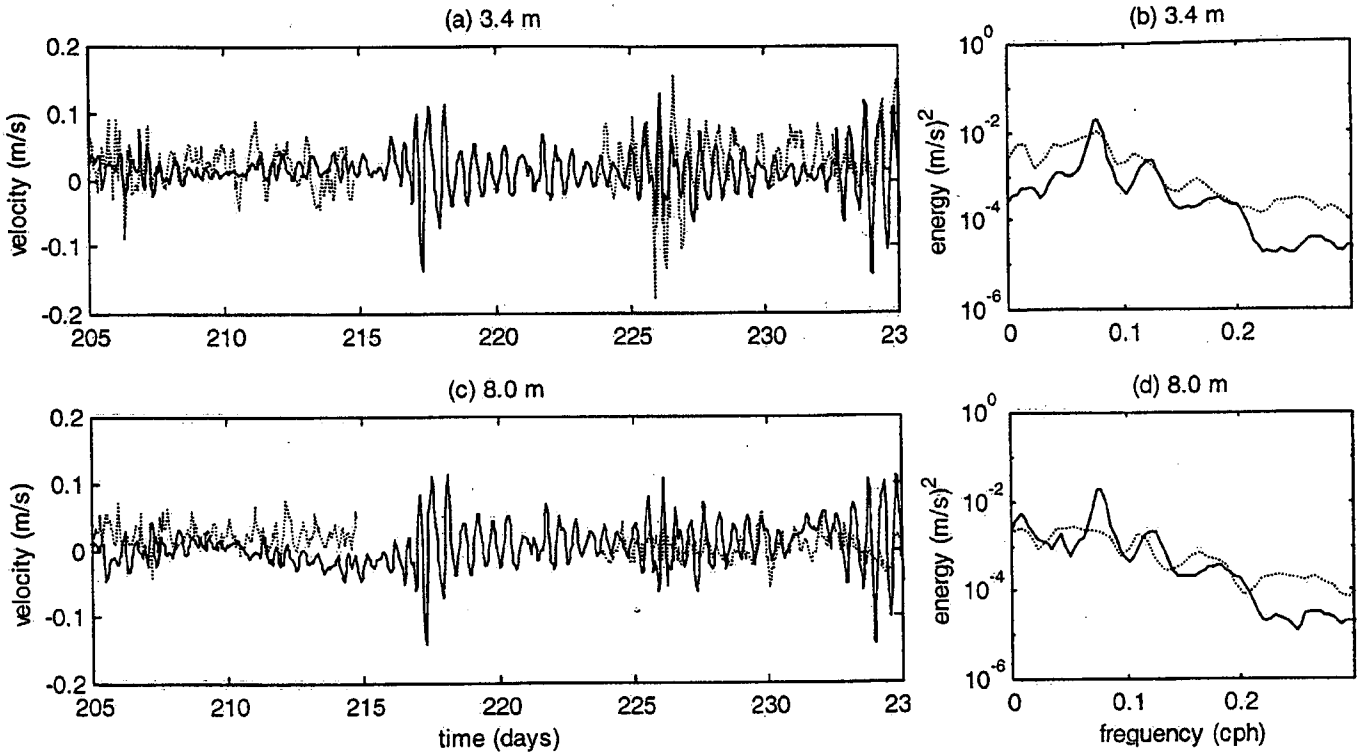

Figure 7: Boegman, Loewen, Hamblin, Culver and Charlton

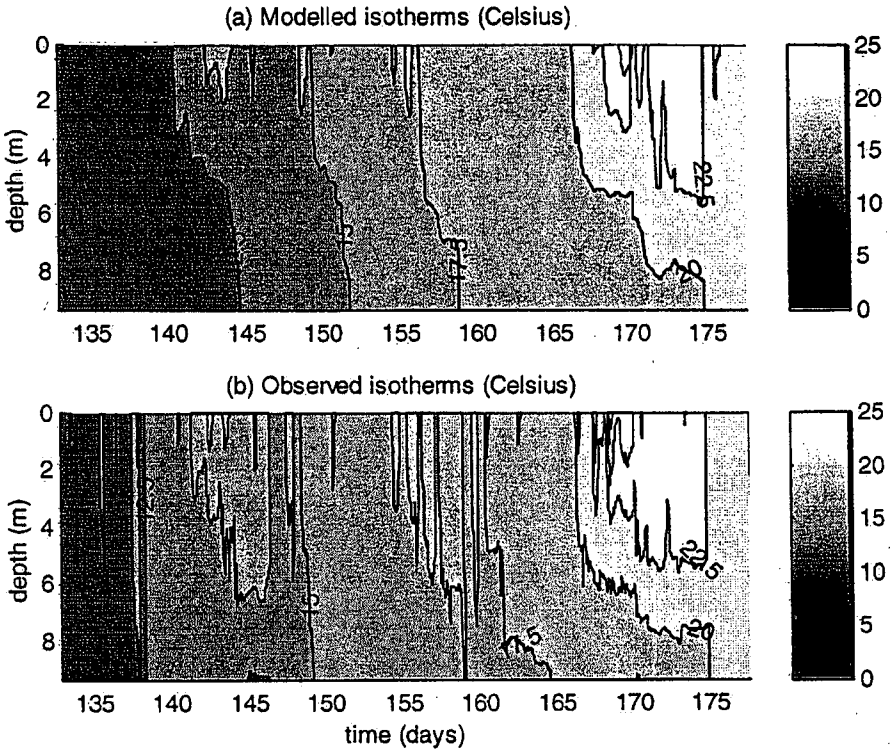

Figure 8: Boegman, Loewen, Hamblin, Culver and Charlton

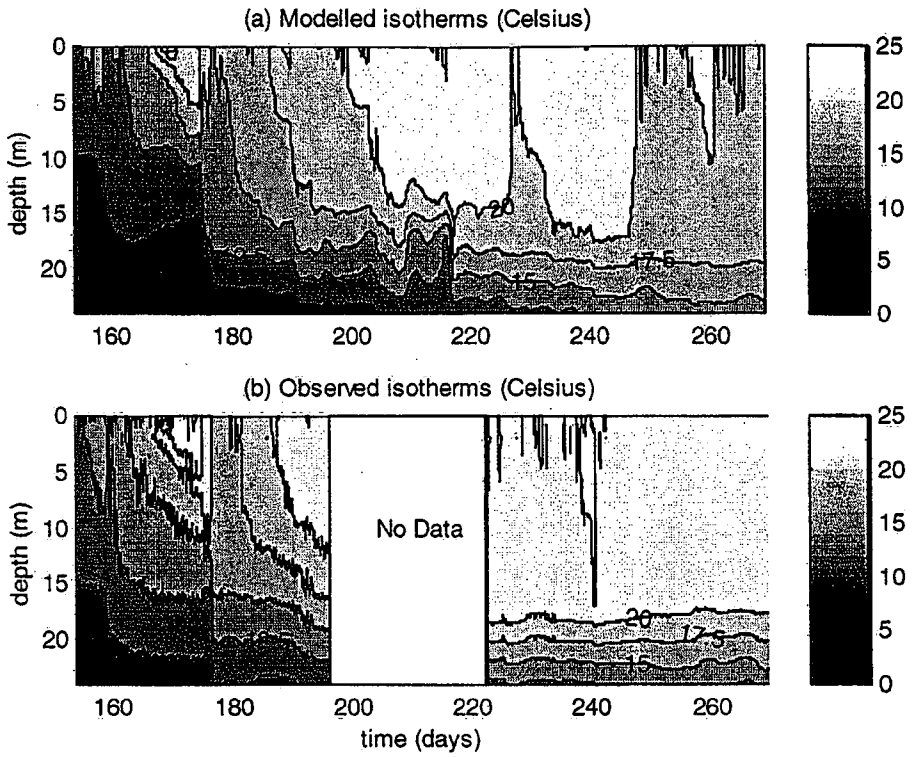

Figure 9: Boegman, Loewen, Hamblin, Culver and Charlton

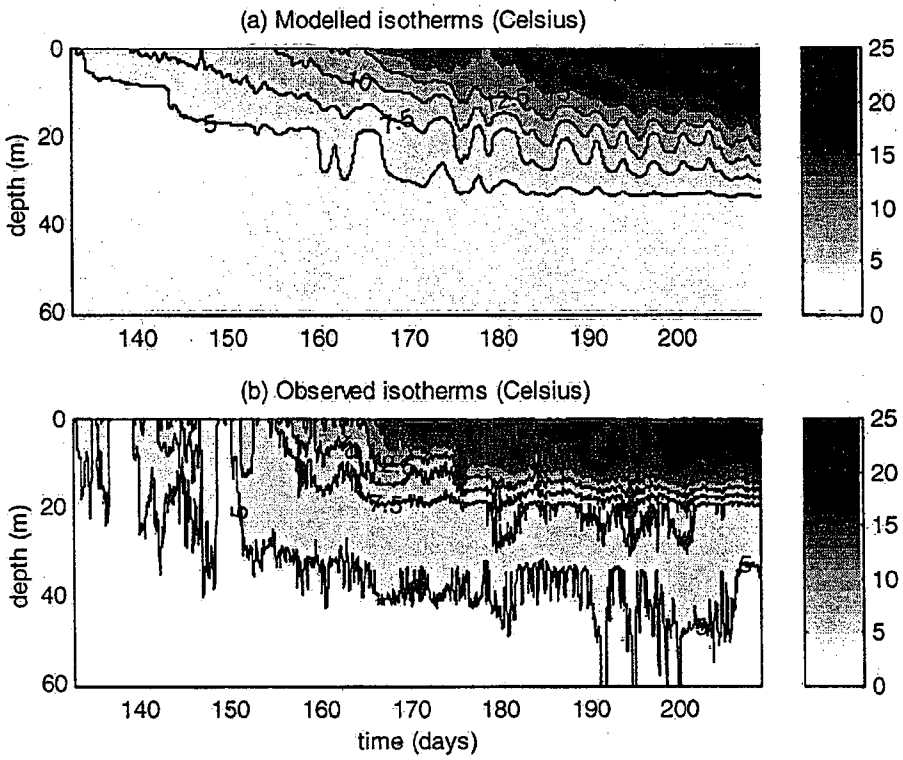

Figure 10: Boegman, Loewen, Hamblin, Culver and Charlton

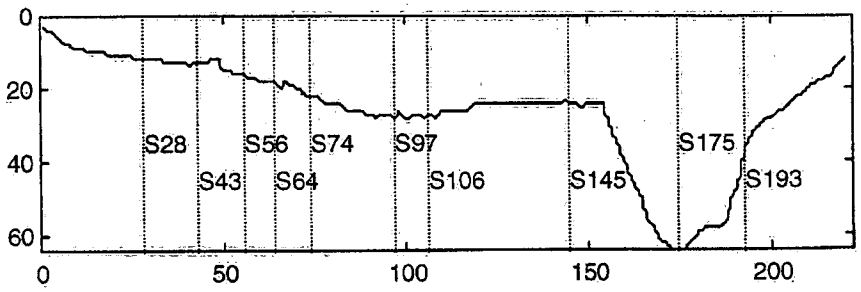

Figure 11-a: Boegman, Loewen, Hamblin, Culver and Charlton

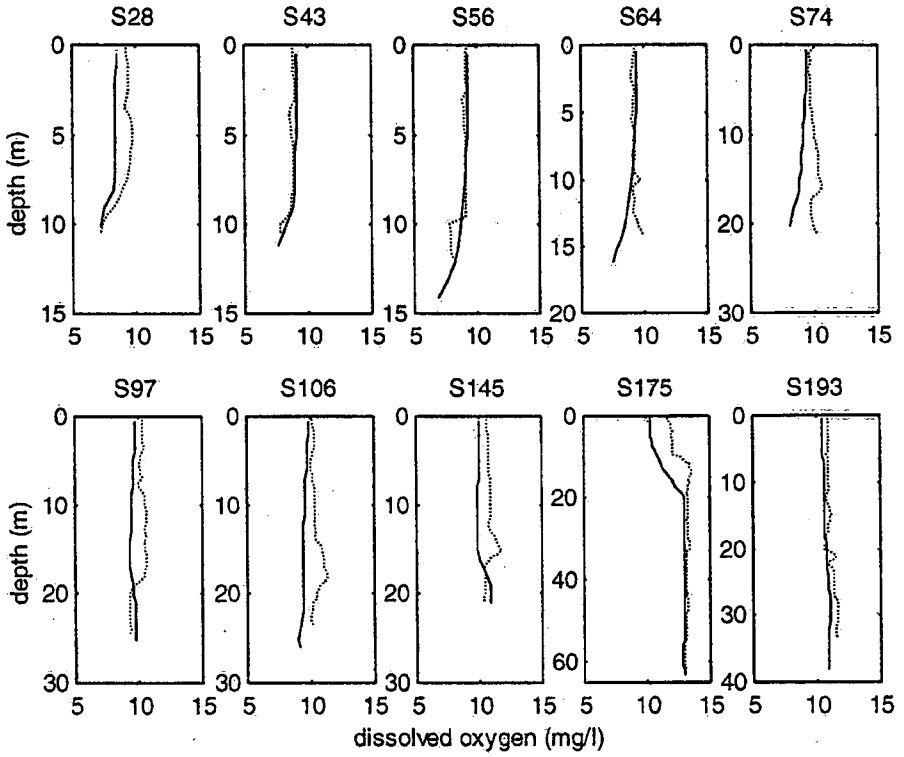

Figure 11-b: Boegman, Loewen, Hamblin, Culver and Charlton

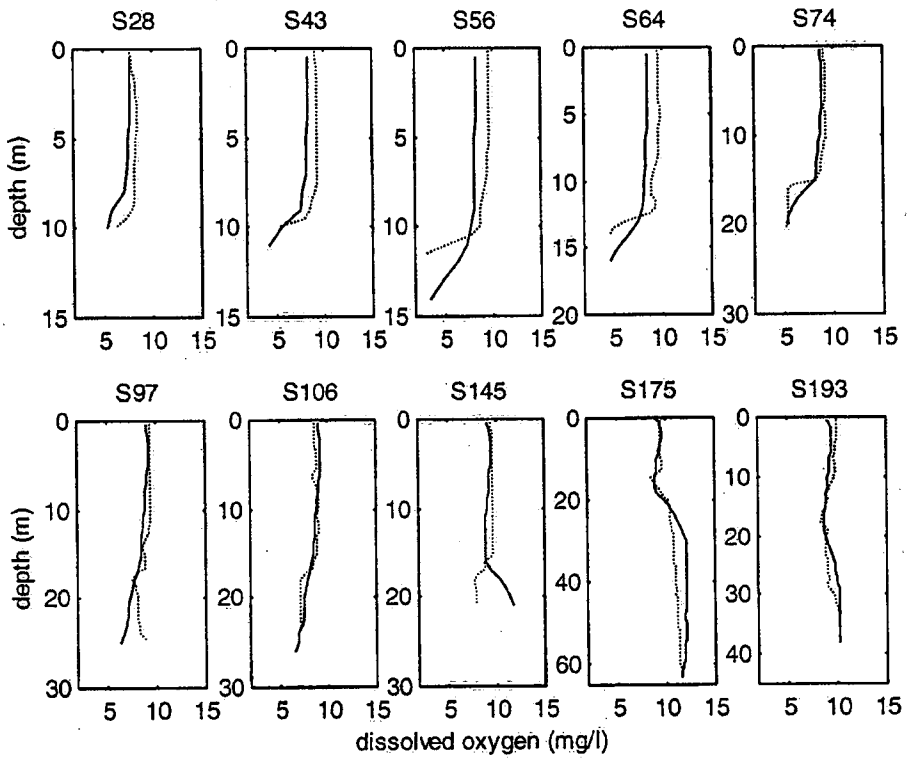

Figure 11-c: Boegman, Loewen, Hamblin, Culver and Charlton

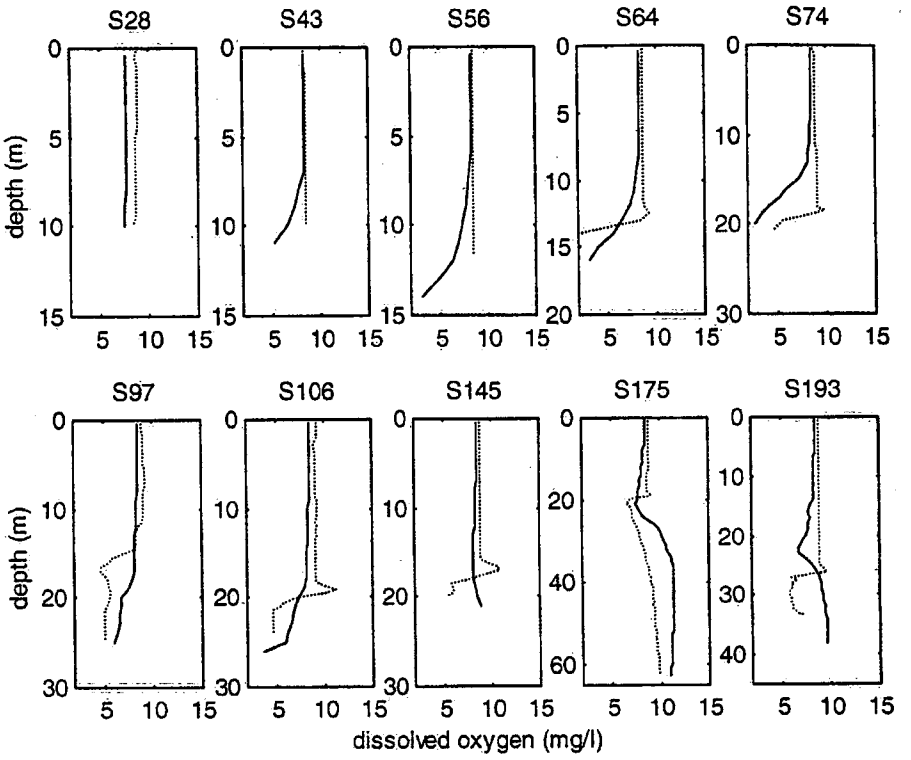

Figure 11-d: Boegman, Loewen, Hamblin, Culver and Charlton

Environment Canada Environnement Canada

Canada

Canada Centre for Inland Waters
P.O. Box 5050
867 Lakeshore Road
Burlington, Ontario
L7R 4A6 Canada

National Hydrology Research Centre
11 Innovation Boulevard
Saskatoon, Saskatchewan
S7N 3H5 Canada

St. Lawrence Centre
105 McGill Street
Montreal, Quebec
H2Y 2E7 Canada

Place Vincent Massey
351 St. Joseph Boulevard
Gatineau, Quebec
K1A 0H3 Canada

Centre canadien des eaux intérieures
Case postale 5050
867, chemin Lakeshore
Burlington (Ontario)
L7R 4A6 Canada

Centre national de recherche en hydrologie
11, boul. Innovation
Saskatoon (Saskatchewan)
S7N 3H5 Canada

Centre Saint-Laurent
105, rue McGill
Montréal (Québec)
H2Y 2E7 Canada

Place Vincent-Massey
351 boul. St-Joseph
Gatineau (Québec)
K1A 0H3 Canada